Supporting information

Discovering Two-dimensional Lead-free Perovskite Solar Absorbers via Cation Transmutation

Ming Chen,[a,b] Zhicheng Shan,[b] Xiaofeng Dong,[b] Shengzhong(Frank) Liu,[a,c*] Zhuo Xu[a*]

a. Key Laboratory of Applied Surface and Colloid Chemistry, National Ministry of Education, Shaanxi Engineering Lab for Advanced Energy Technology, School of Materials Science and Engineering, Shaanxi Normal University, Xi'an, China, 710119.

b. School of Electric Power, Civil Engineering and Architecture, School of Physics and Electronics Engineering, State Key Laboratory of Quantum Optics and Quantum Optics Devices, Shanxi University, Taiyuan, China, 030006.

c. State Key Laboratory of Catalysis, Dalian National Laboratory for Clean Energy, Dalian Institute of Chemical Physics, Chinese Academy of Sciences, Dalian, China, 116023.

Corresponding authors*: xuzh@snnu.edu.cn (X. Z.); szliu@dicp.ac.cn (S. Z. L)

Calculation details

The density-functional theory (DFT) calculations were conducted with the Vienna Ab Initio Simulation Package (VASP). The core and valence electronic interactions were described with the frozen-core projector augmented-wave (PAW) potentials. The exchange correlation energy was described with the Perdew-Burke-Ernzerhof (PBE) in generalized gradient approximation (GGA). An energy cutoff of 400 eV was used for the plane-wave function's expansion. Energy convergence of electronic calculations adopted the tolerance of 10^{-5} eV. The residual forces on atoms was set to converge to below 0.02 eV/Å. The DFT-D3 method was used to describe van der Waals (vdW) interaction. A Γ-centered k-point sampling of 3×3×3 for Brillouin zone integration was generated using the Monkhorst-Pack scheme. Because of the HSE+SOC functional are very costly, so we first considered the band structures with complicate K-path using the PBE+SOC functional. As the direct and indirect characteristics and locations of VBM and CBM are determined, we use a simple K-path for direct band structures calculation using the HSE+SOC functional. While the complicate K-path is used for the indirect band structures calculation using the HSE+SOC functional. Dielectric constants were calculated using the density functional perturbation theory (DFPT) method. We used the package LOBSTER to compute the crystal orbital Hamiltonian populations (COHP) for the bonding analysis, which is calculated based on PBE scheme. The optical absorption spectra are calculated using the PBE+SOC scheme, and corrected to match with the HSE06+SOC value using the scissor operator. The theoretical maximum PCE is evaluated using the "spectroscopic limited maximum efficiency" (SLME) method.

Table S1. The optimized lattice constants and calculated band gaps (eV) for 2D double perovskites $BDA_2M_IM_{III}Cl_8$ (M_I = Na^+, K^+, Rb^+, Cu^+, Ag^+, and Au^+; M_{III} = Bi^{3+}, In^{3+}, and Sb^{3+}) using the PBE, PBE+SOC, and HSE06 + SOC schemes. The "I" in bracket denotes that it belong to indirect band gap type, and "D" in bracket denotes that it belong to direct band gap type.

	Compounds	Lattice constant (Å)			Band gap (eV)		
		a (Å)	*b* (Å)	*c* (Å)	PBE	PBE+SOC	HSE06+SOC
Cl	$BDA_2NaBiCl_8$	7.62	7.83	9.38	4.09 (I)	3.18 (I)	4.14
	$BDA_2NaInCl_8$	7.56	7.71	9.29	3.49 (I)	3.48 (I)	4.82
	$BDA_2NaSbCl_8$	7.58	7.79	9.35	3.49 (I)	3.28 (I)	4.24
	BDA_2KBiCl_8	7.64	7.98	9.57	4.20 (I)	3.23 (I)	4.19
	BDA_2KInCl_8	7.59	7.86	9.48	3.45 (I)	3.45 (I)	4.82
	BDA_2KSbCl_8	7.61	7.93	9.69	3.61 (I)	3.35 (I)	4.23
	$BDA_2RbBiCl_8$	7.67	8.05	9.63	4.04 (I)	3.13 (I)	4.22
	$BDA_2RbInCl_8$	7.61	7.93	9.56	3.35 (I)	3.34 (I)	4.71
	$BDA_2RbSbCl_8$	7.66	8.01	9.60	3.56 (I)	3.32 (I)	4.21
	$BDA_2CuBiCl_8$	7.70	7.91	8.99	2.20 (I)	1.34 (D)	2.44
	$BDA_2CuInCl_8$	7.62	7.81	8.90	1.80 (I)	1.78 (I)	3.13
	$BDA_2CuSbCl_8$	7.63	7.81	9.16	2.11 (I)	1.86 (D)	3.00
	$BDA_2AgBiCl_8$	7.71	7.92	9.14	2.86 (I)	2.06 (D)	3.10
	$BDA_2AgInCl_8$	7.66	7.80	9.06	2.46 (I)	2.45 (I)	3.68
	$BDA_2AgSbCl_8$	7.70	7.87	9.12	2.64 (I)	2.52 (D)	3.53
	$BDA_2AuBiCl_8$	7.83	8.12	8.96	2.93 (I)	2.01 (D)	2.95
	$BDA_2AuInCl_8$	7.77	7.96	8.89	2.64 (I)	2.50 (I)	3.66
	$BDA_2AuSbCl_8$	7.81	8.05	8.93	2.63 (I)	2.41 (D)	3.32

Table S2. The optimized lattice constants and calculated band gaps (eV) for 2D double perovskites $BDA_2M_IM_{III}Br_8$ (M_I = Na^+, K^+, Rb^+, Cu^+, Ag^+, and Au^+; M_{III} = Bi^{3+}, In^{3+}, and Sb^{3+}) using the PBE, PBE+SOC, and HSE06 + SOC schemes. The "I" in bracket denotes that it belong to indirect band gap type , and "D" in bracket denotes that it belong to direct band gap type.

	Material	Lattice constant (Å)			Bandgap (eV)		
		a (Å)	*b* (Å)	*c* (Å)	PBE	PBE+SOC	HSE06+SOC
Br	$BDA_2NaBiBr_8$	7.91	8.06	9.56	3.49 (I)	2.63 (I)	3.48
	$BDA_2NaInBr_8$	7.89	7.93	9.48	2.65 (I)	2.56 (I)	3.65
	$BDA_2NaSbBr_8$	7.89	8.03	9.54	3.03 (I)	2.84 (I)	3.61
	BDA_2KBiBr_8	7.93	8.22	9.74	3.37 (I)	2.52 (I)	3.49
	BDA_2KInBr_8	7.90	8.11	9.66	2.51 (I)	2.46 (I)	3.59
	BDA_2KSbBr_8	7.92	8.19	9.70	3.13 (I)	2.91 (I)	3.69
	$BDA_2RbBiBr_8$	7.95	8.30	9.76	3.20 (I)	2.40 (I)	3.38
	$BDA_2RbInBr_8$	7.91	8.18	9.75	2.39 (I)	2.36 (I)	3.48
	$BDA_2RbSbBr_8$	7.92	8.28	9.78	3.07 (I)	2.89 (I)	3.65
	$BDA_2CuBiBr_8$	7.95	8.07	9.23	1.84 (I)	1.09 (D)	2.03
	$BDA_2CuInBr_8$	7.87	7.98	9.19	1.24 (I)	1.24 (I)	2.33
	$BDA_2CuSbBr_8$	7.93	8.02	9.21	1.72 (I)	1.52 (D)	2.48
	$BDA_2AgBiBr_8$	7.98	8.09	9.37	2.33 (I)	1.66 (D)	2.48
	$BDA_2AgInBr_8$	7.92	8.01	9.30	1.82 (I)	1.81 (I)	2.83
	$BDA_2AgSbBr_8$	7.95	8.05	9.36	2.13 (I)	2.05 (D)	2.89
	$BDA_2AuBiBr_8$	8.09	8.25	9.18	2.18 (I)	1.47 (D)	2.20
	$BDA_2AuInBr_8$	8.02	8.12	9.14	1.77 (I)	1.70 (I)	2.62
	$BDA_2AuSbBr_8$	8.06	8.21	9.15	1.95 (I)	1.83 (D)	2.59

Table S3. The optimized lattice constants and calculated band gaps (eV) for 2D double Perovskites $BDA_2M_IM_{III}I_8$ (M_I = Na^+, K^+, Rb^+, Cu^+, Ag^+, and Au^+; M_{III} = Bi^{3+}, In^{3+}, and Sb^{3+}) using the PBE, PBE+SOC, and HSE06 + SOC schemes. The "I" in bracket denotes that it belong to indirect band gap type , and "D" in bracket denotes that it belong to direct band gap type.

	Material	Lattice constant (Å)			Bandgap (eV)		
		a (Å)	*b* (Å)	*c* (Å)	PBE	PBE+SOC	HSE06+SOC
I	BDA_2NaBiI_8	8.32	8.41	9.86	2.73 (I)	1.91 (I)	2.62
	BDA_2NaInI_8	8.20	8.28	9.91	1.66 (I)	1.53 (I)	2.32
	BDA_2NaSbI_8	8.34	8.37	9.79	2.46 (I)	2.22 (I)	2.85
	BDA_2KBiI_8	8.35	8.54	10.01	2.42 (I)	1.71 (I)	2.45
	BDA_2KInI_8	8.33	8.41	9.97	1.53 (I)	1.43 (I)	2.28
	BDA_2KSbI_8	8.33	8.51	9.99	2.33 (I)	2.12 (I)	2.91
	BDA_2RbBiI_8	8.37	8.61	10.06	2.33 (I)	1.57 (I)	2.31
	BDA_2RbInI_8	8.34	8.49	10.06	1.36 (D)	1.29 (D)	2.13
	BDA_2RbSbI_8	8.35	8.57	10.07	2.13 (I)	1.96 (I)	2.76
	BDA_2CuBiI_8	8.24	8.31	9.74	1.49 (I)	0.87 (D)	1.58
	BDA_2CuInI_8	8.26	8.31	9.54	0.68 (I)	0.69 (I)	1.46
	BDA_2CuSbI_8	8.31	8.35	9.54	1.43 (I)	1.26 (D)	1.97
	BDA_2AgBiI_8	8.37	8.43	9.69	1.82 (I)	1.24 (D)	1.84
	BDA_2AgInI_8	8.30	8.36	9.64	1..00 (I)	1.00 (I)	1.89
	BDA_2AgSbI_8	8.33	8.40	9.66	1.64 (I)	1.56 (D)	2.23
	BDA_2AuBiI_8	8.45	8.52	9.55	1.47 (I)	1.01 (D)	1.54
	BDA_2AuInI_8	8.39	8.42	9.50	0.85 (I)	0.83 (I)	1.46
	BDA_2AuSbI_8	8.41	8.48	9.51	1.29 (I)	1.22 (D)	1.87

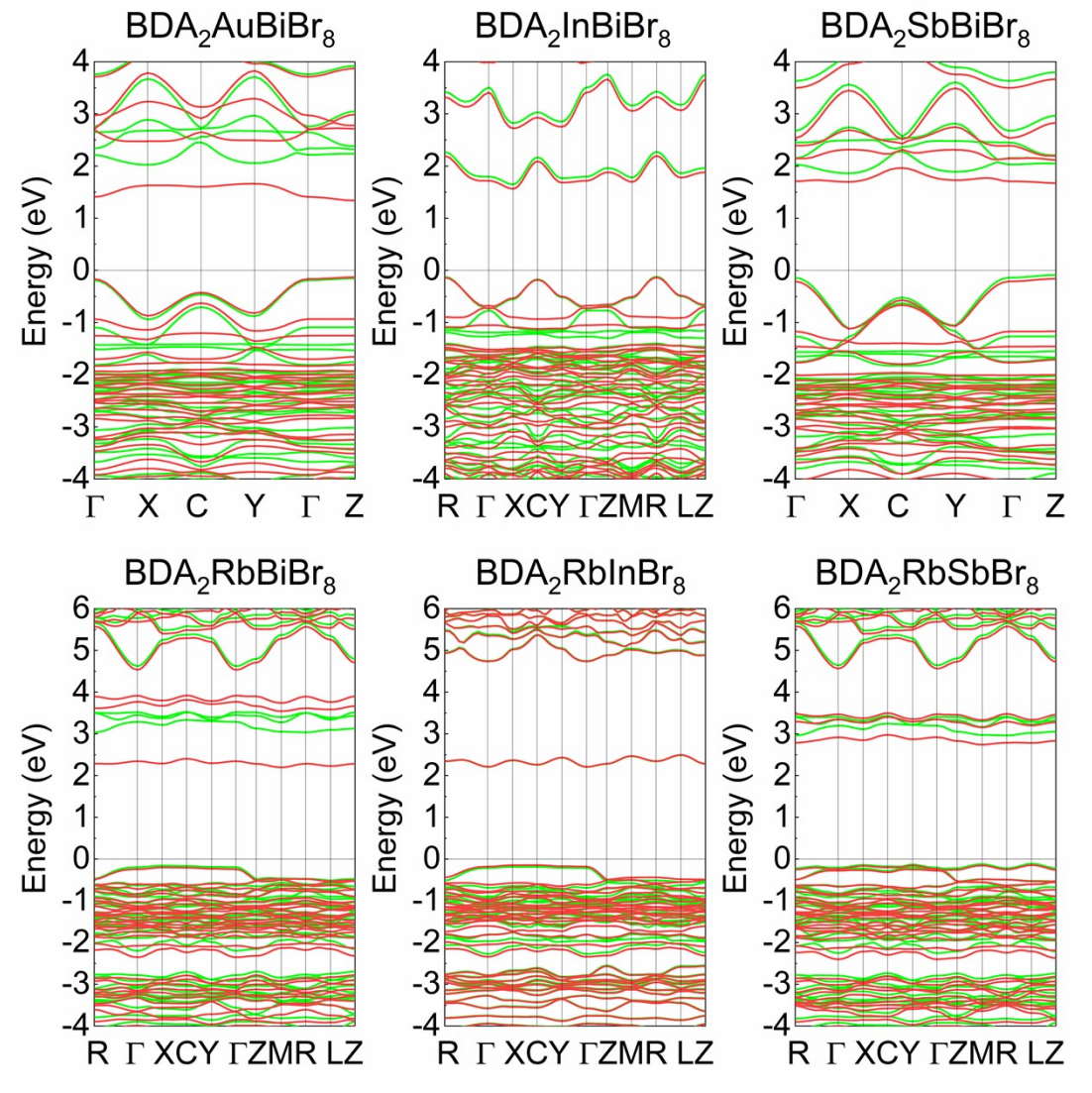

Fig. S1. Calculated band structures of several representative 2D double perovskites using PBE (green) and PBE+SOC (red) schemes, respectively.

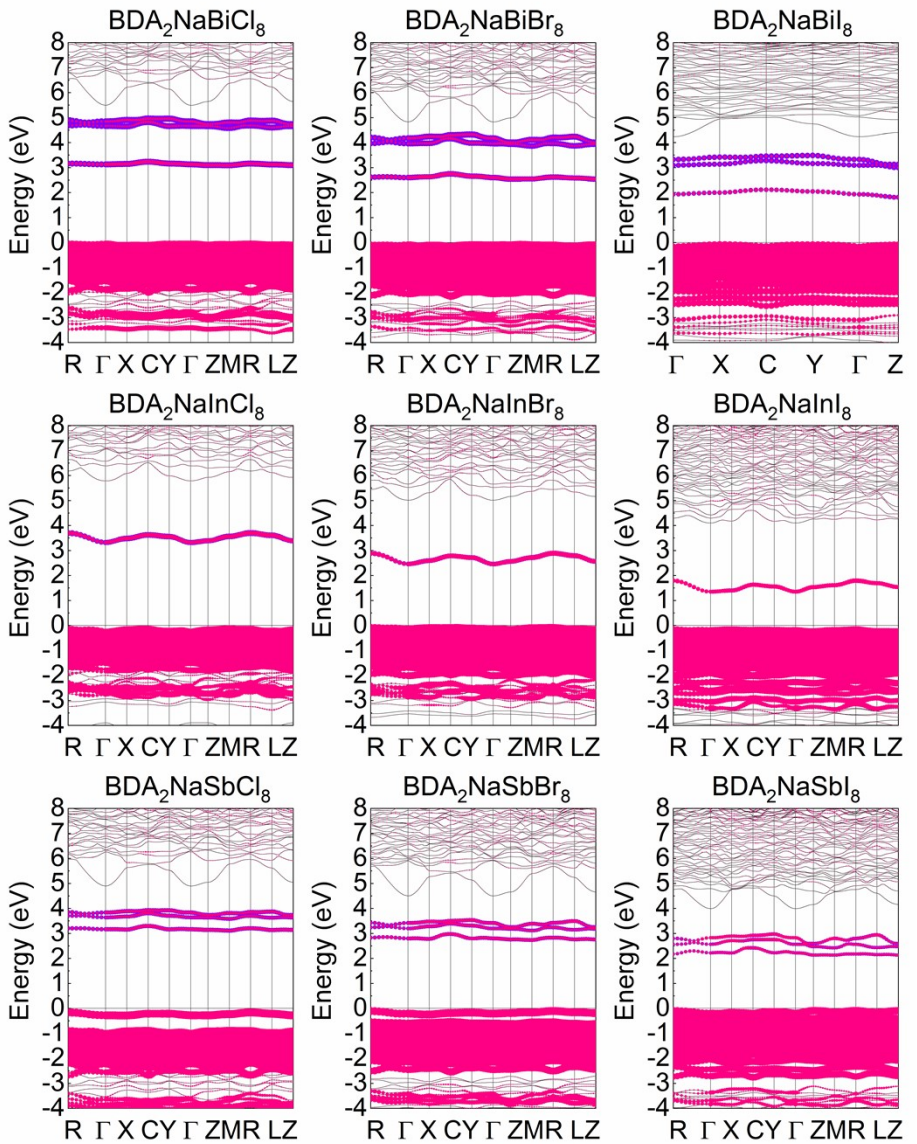

Fig. S2. Orbital projected band structures of Na-based 2D double perovskites (the pink lines represent the halide p states; the violet lines represent the Bi 6p, In 5s, and Sb 5p states in BDA_2NaBiX_8, BDA_2NaInX_8, and BDA_2NaSbX_8, respectively).

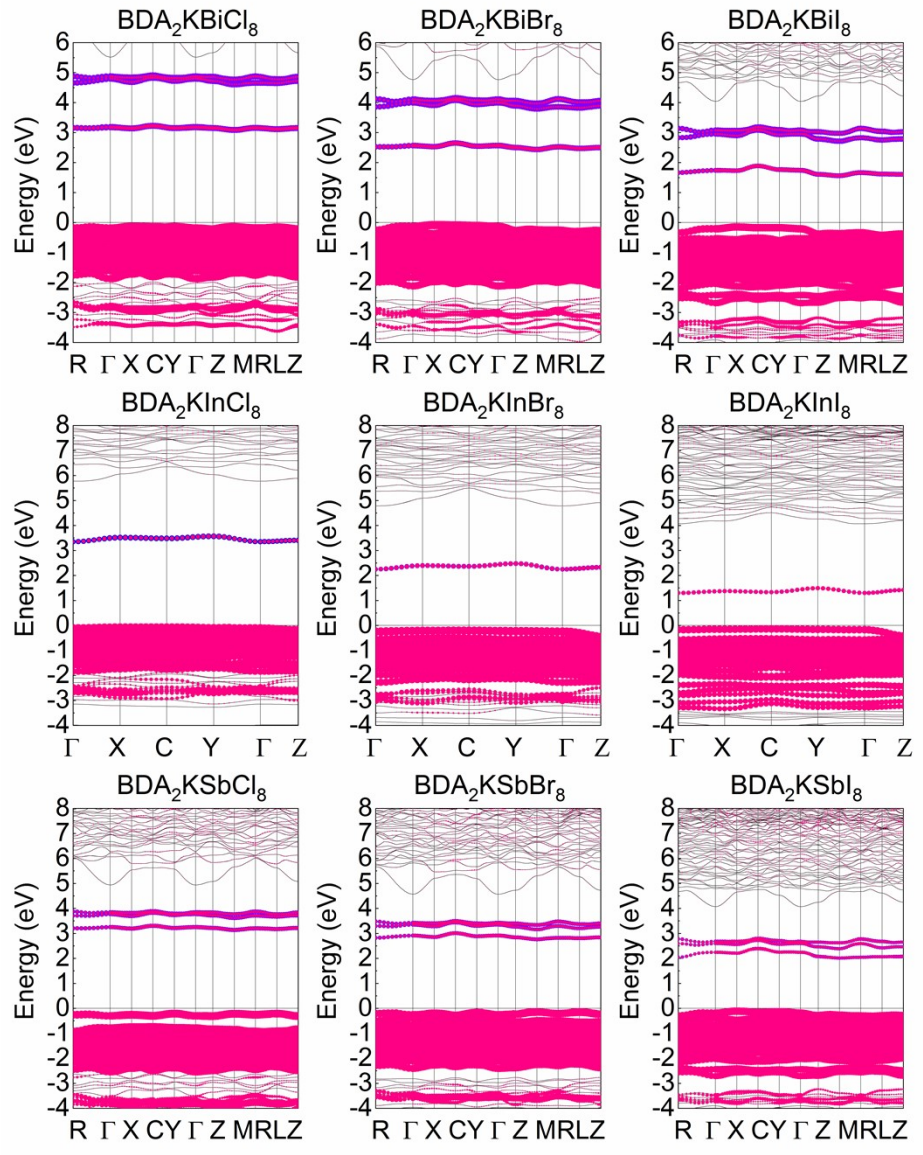

Fig. S3. Orbital projected band structures of K-based 2D double perovskites (the pink lines represent the halide p states; the violet lines represent the Bi 6p, In 5s, and Sb 5p states in BDA_2KBiX_8, BDA_2KInX_8, and BDA_2KSbX_8, respectively).

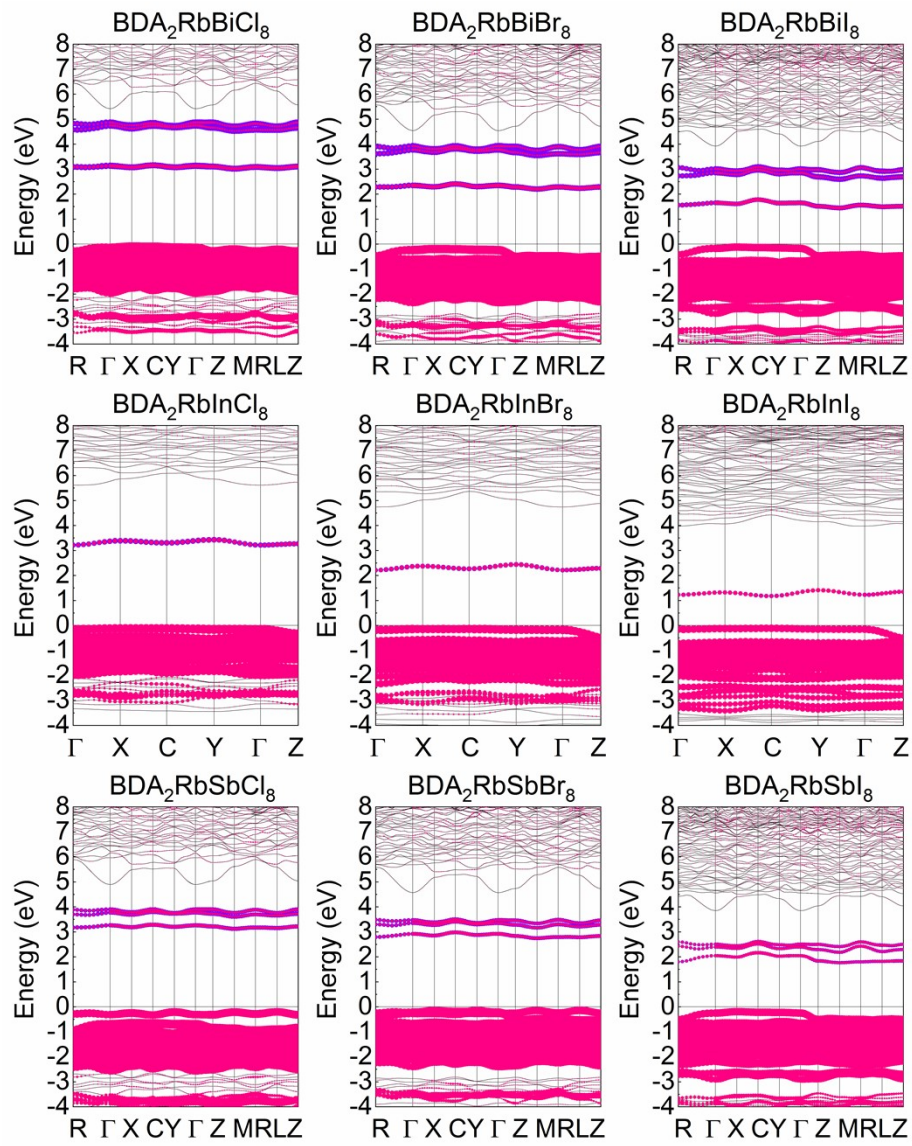

Fig. S4. Orbital projected band structures of Rb-based 2D double perovskites (the pink lines represent the halide p states; the violet lines represent the Bi 6p, In 5s, and Sb 5p states in BDA_2RbBiX_8, BDA_2RbBiX_8, and BDA_2RbBiX_8, respectively).

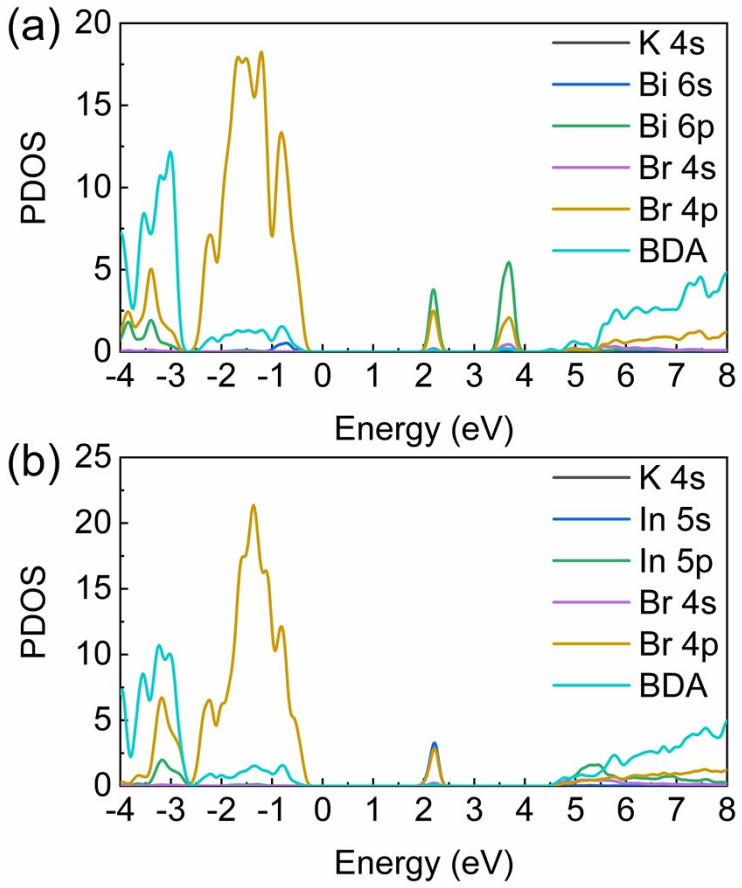

Fig. S5. Calculated projected density of states (PDOS) of (a) BDA_2KBiBr_8 and (b) BDA_2KInBr_8 based on PBE+SOC scheme.

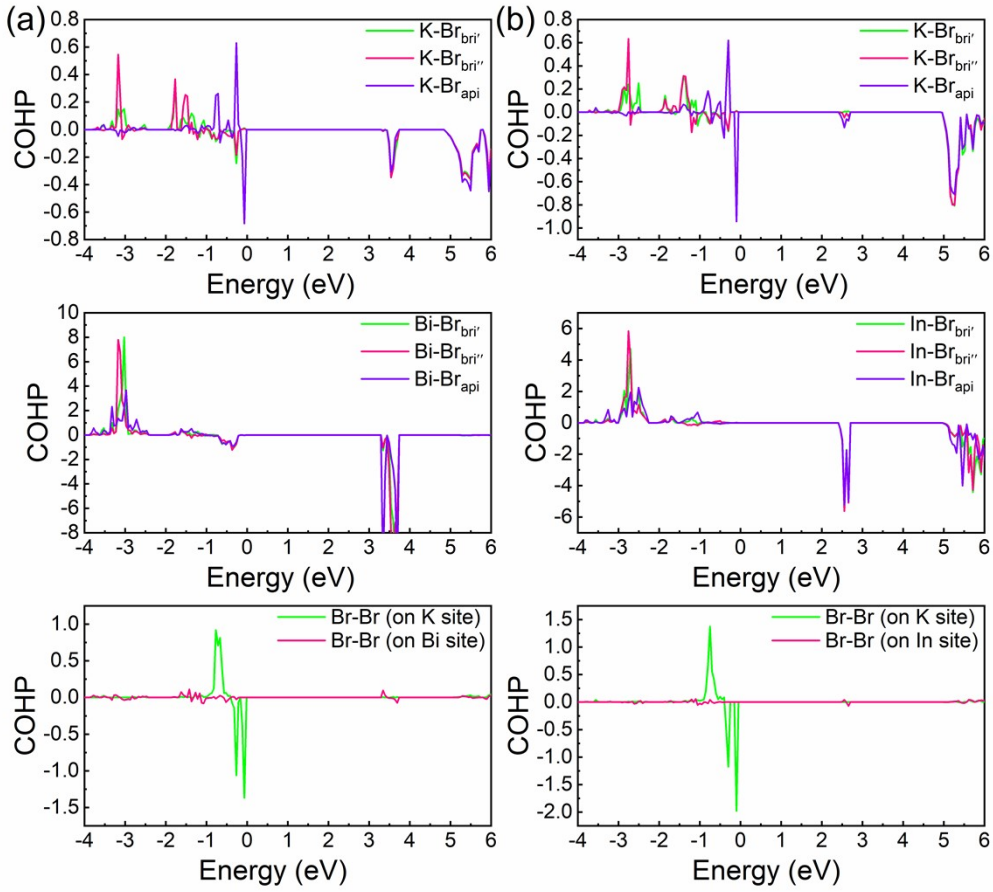

Fig. S6. The projected crystal orbital Hamilton population (pCOHP) analysis of (a) K-Br, Bi-Br, and apical Br-Br bonding interactions in BDA_2KBiBr_8 and (b) K-Br, In-Br, and apical Br-Br bonding interactions inBDA_2KInBr_8.

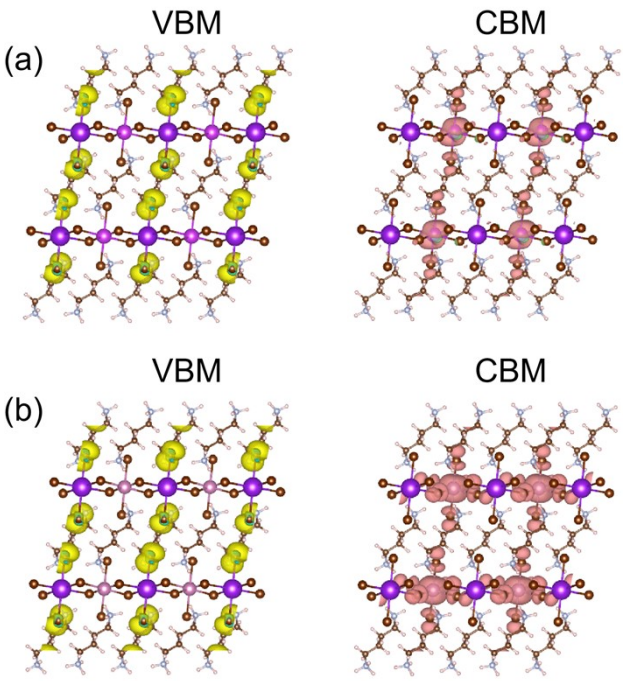

Fig. S7. The valence band maximum (VBM) and conduction band minimum (CBM) of (a) BDA_2KBiBr_8 and (b) BDA_2KInBr_8 based on PBE+SOC scheme.

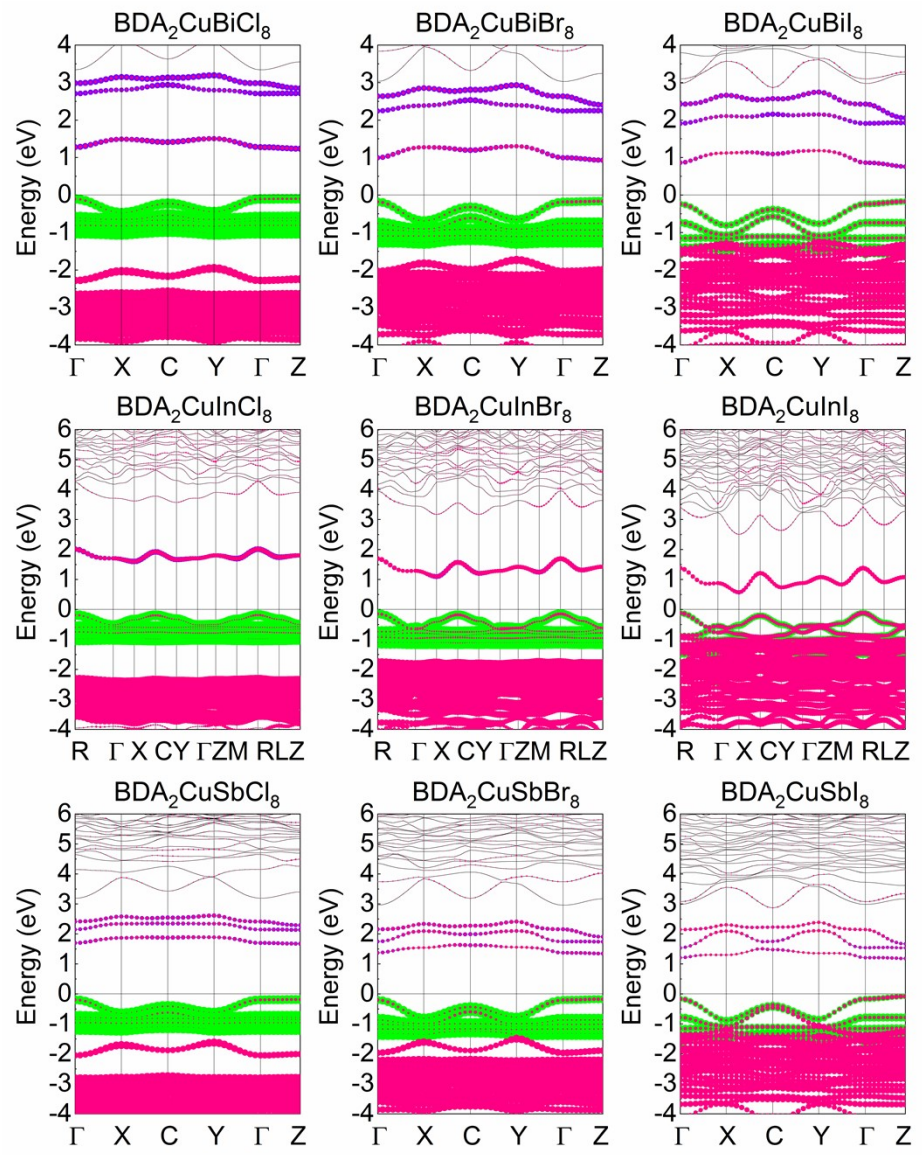

Fig. S8. Orbital projected band structures of Cu-based 2D double perovskites (the green and pink lines represent the Cu 3d and halide p states; the violet lines represent the Bi 6p, In 5s, and Sb 5p states in BDA_2CuBiX_8, BDA_2CuInX_8, and BDA_2CuSbX_8, respectively).

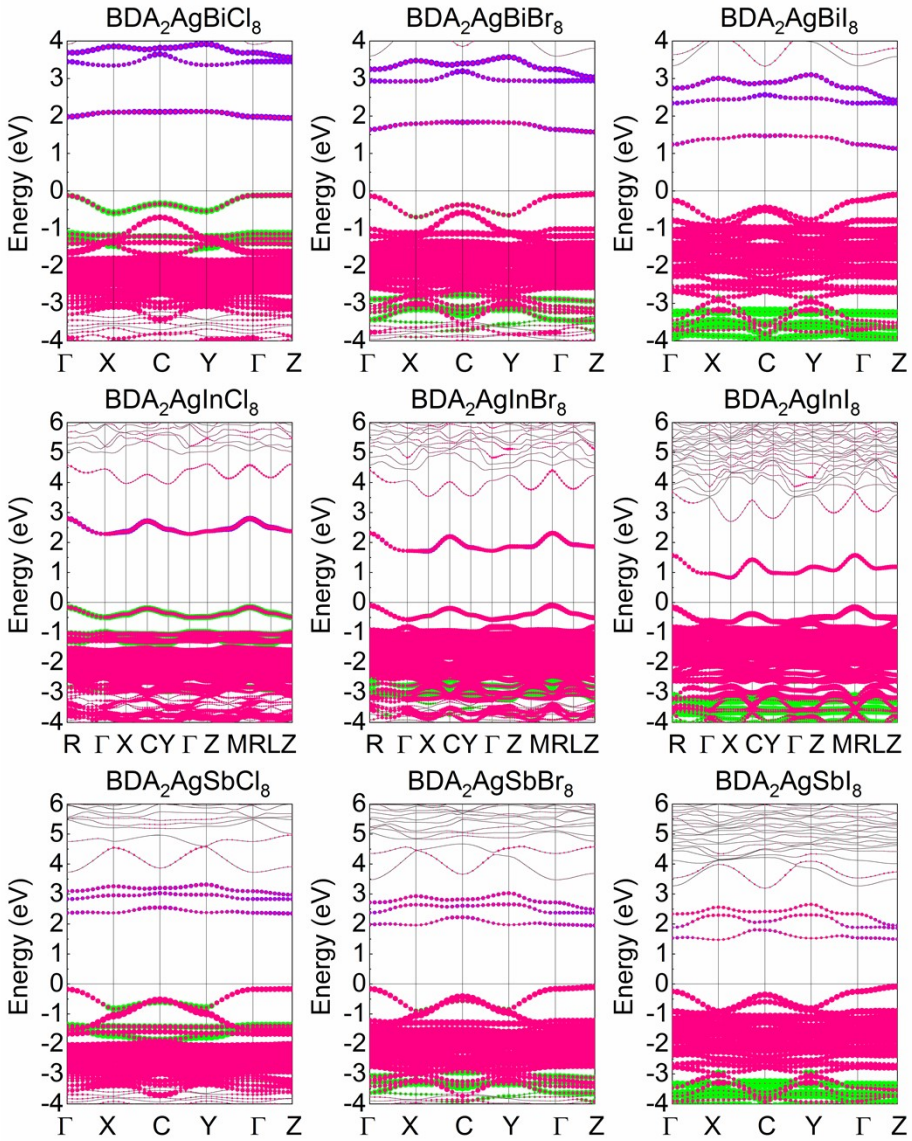

Fig. S9. Orbital projected band structures of Ag-based 2D double perovskites (the green and pink lines represent the Cu 3d and halide p states; the violet lines represent the Bi 6p, In 5s, and Sb 5p states in BDA_2AgBiX_8, BDA_2AgInX_8, and BDA_2AuSbX_8, respectively).

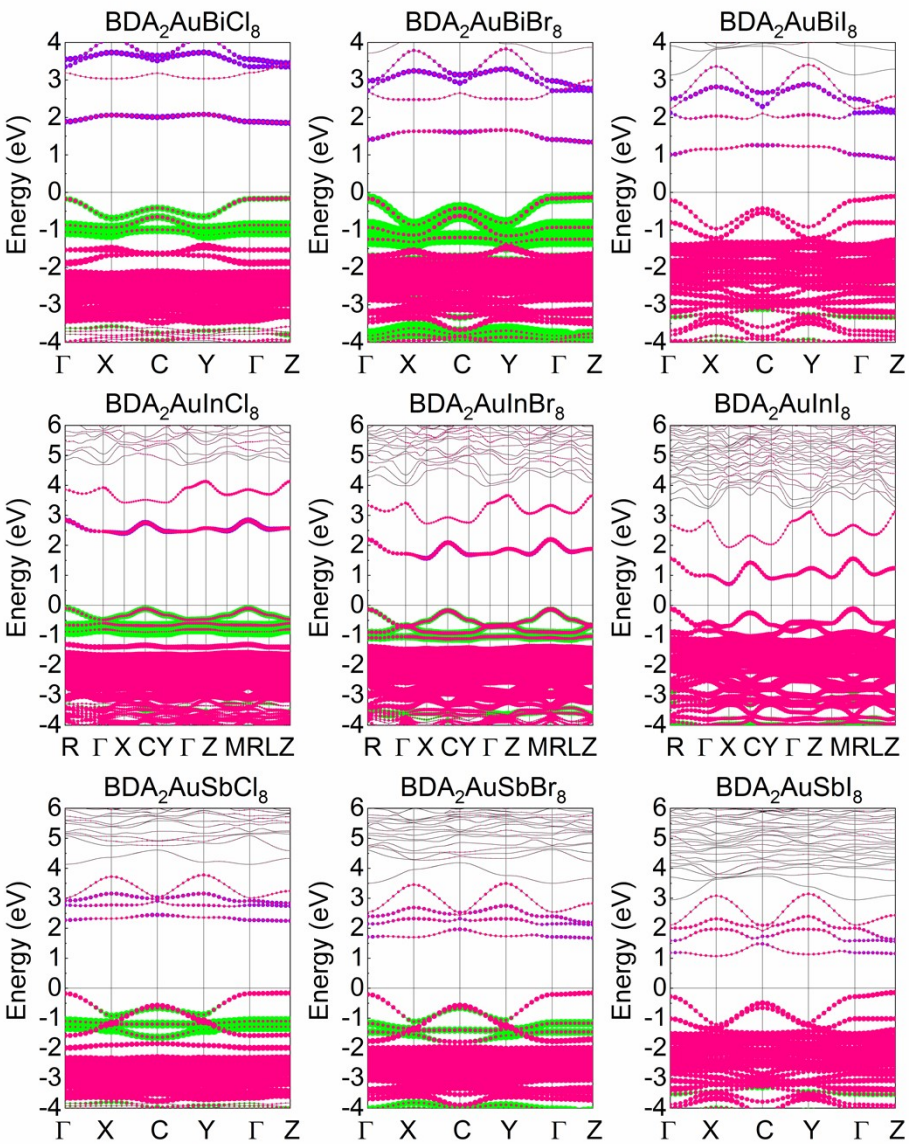

Fig. S10. Orbital projected band structures of Au-based 2D double perovskites (the green and pink lines represent the Cu 3d and halide p states; the violet lines represent the Bi 6p, In 5s, and Sb 5p states in BDA_2AuBiX_8, BDA_2AuInX_8, and BDA_2AuSbX_8, respectively).

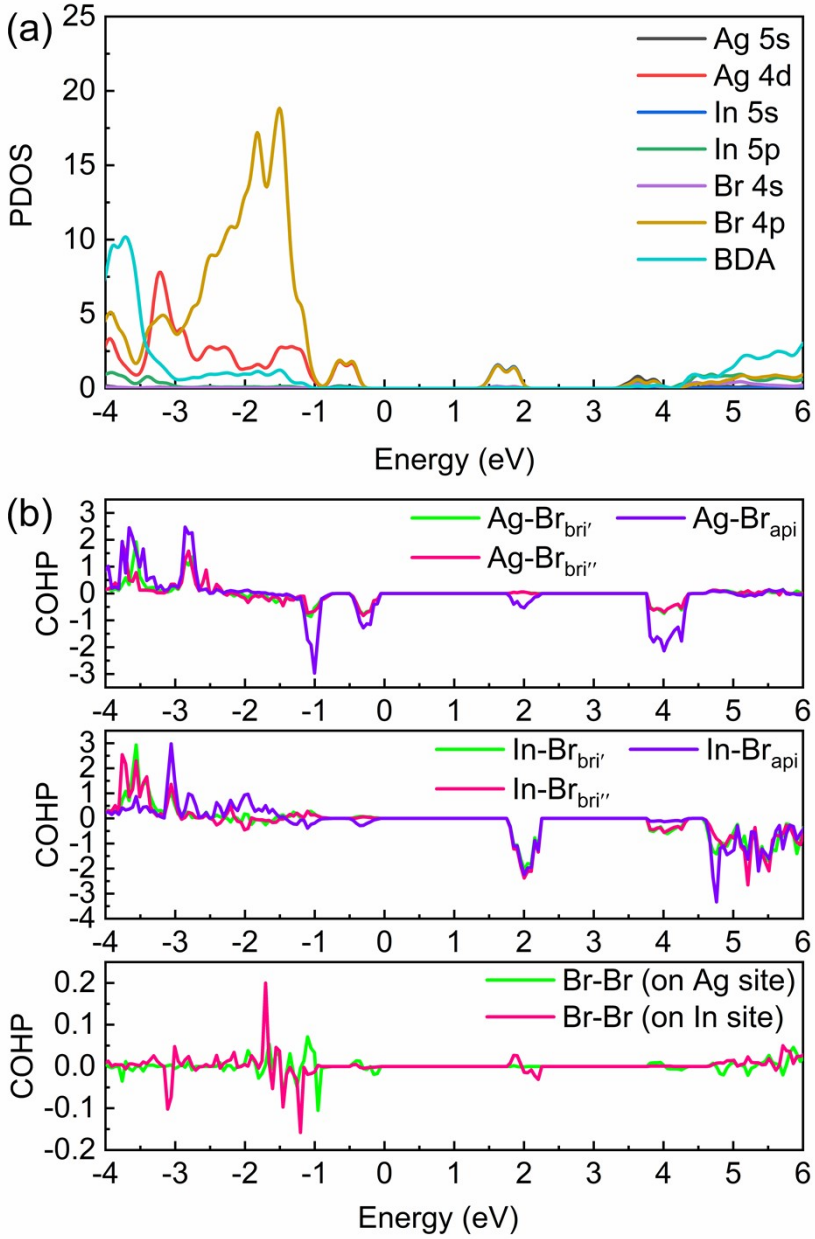

Fig. S11. (a) Calculated projected density of states (PDOS) of $BDA_2AgInBr_8$; and (b) the corresponding projected crystal orbital Hamilton population (pCOHP) analysis of K-Br, Bi-Br, and apical Br-Br bonding interactions in $BDA_2AgInBr_8$ based on PBE+SOC scheme.

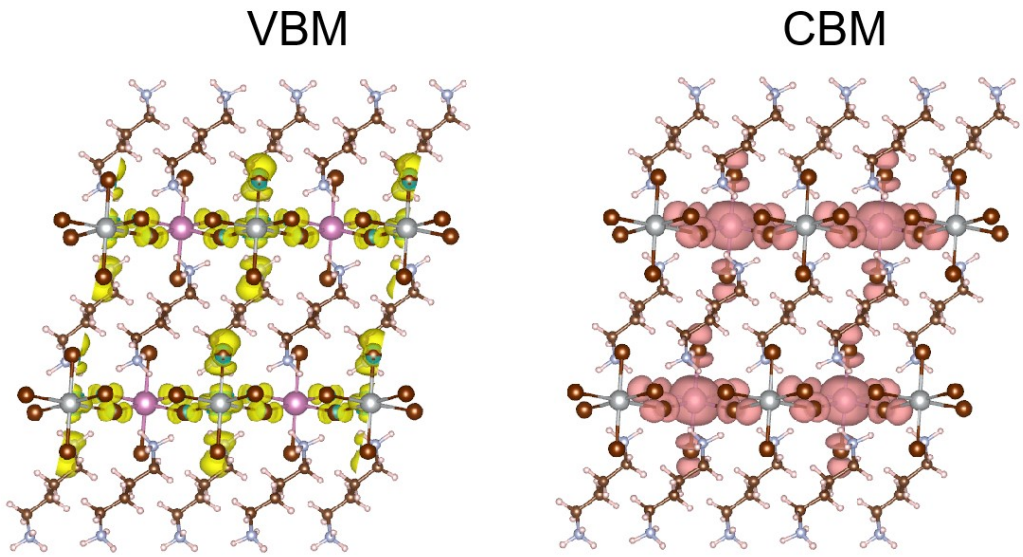

Fig. S12. The valence band maximum (VBM) and conduction band minimum (CBM) of $BDA_2AgInBr_8$ based on PBE+SOC scheme.

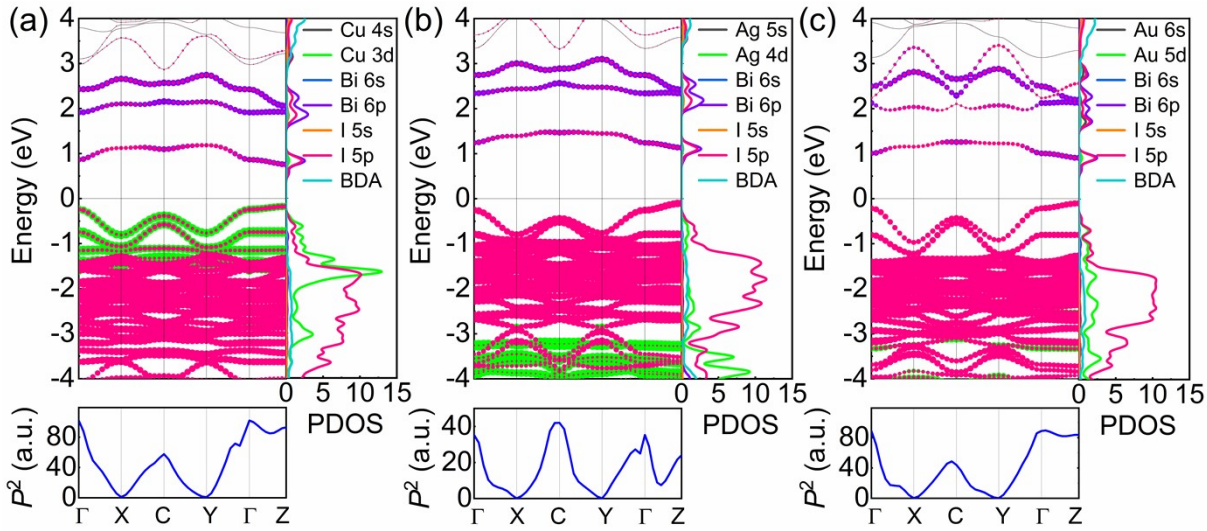

Fig. S13. PBE+SOC calculated band structures, projected density of states (PDOS), and corresponding transition matrix elements (in unit of Debey^2) for (a) BDA_2CuBiI_8, (b) BDA_2AgBiI_8, and (c) BDA_2AuBiI_8.

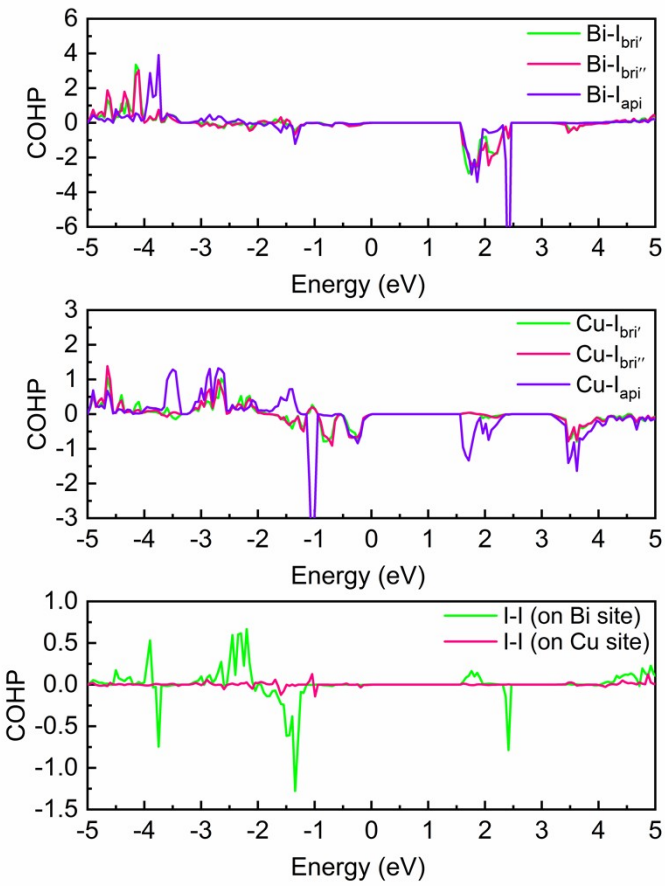

Fig. S14. The projected crystal orbital Hamilton population (pCOHP) analysis of Bi-I, Cu-I, and apical I-I bonding interactions in BDA_2CuBiI_8.

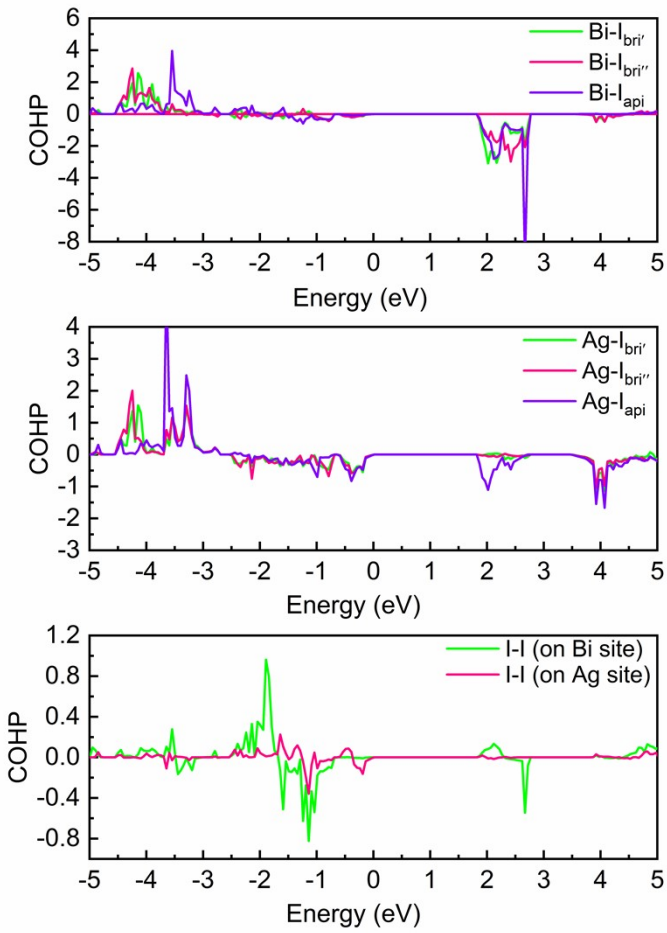

Fig. S15. The projected crystal orbital Hamilton population (pCOHP) analysis of Bi-I, Ag-I, and apical I-I bonding interactions in BDA_2AgBiI_8.

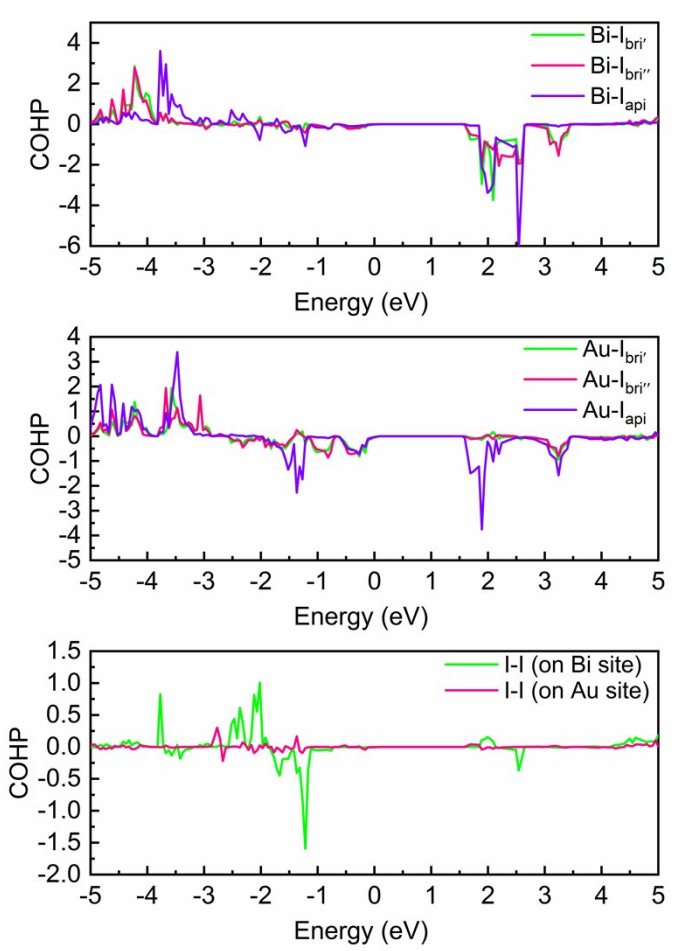

Fig. S16. The projected crystal orbital Hamilton population (pCOHP) analysis of Bi-I, Au-I, and apical I-I bonding interactions in BDA_2AuBiI_8.

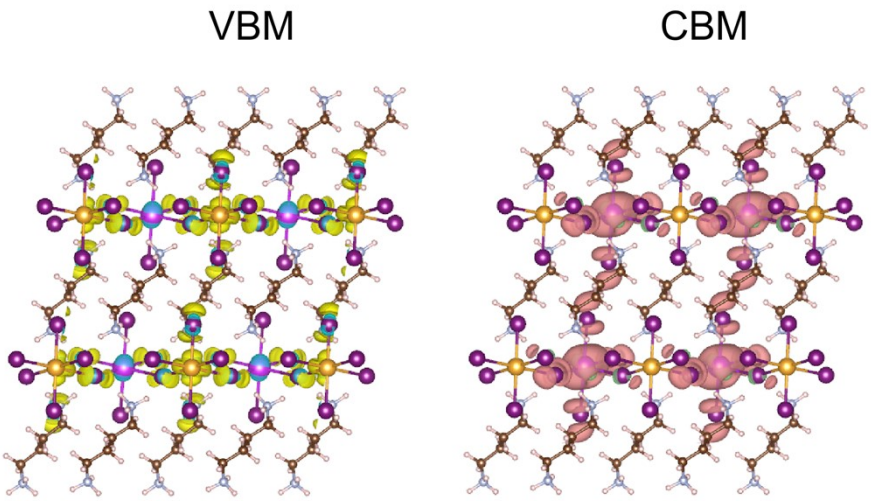

Fig. S17. The valence band maximum (VBM) and conduction band minimum (CBM) of BDA_2AuBiI_8 based on PBE+SOC scheme.

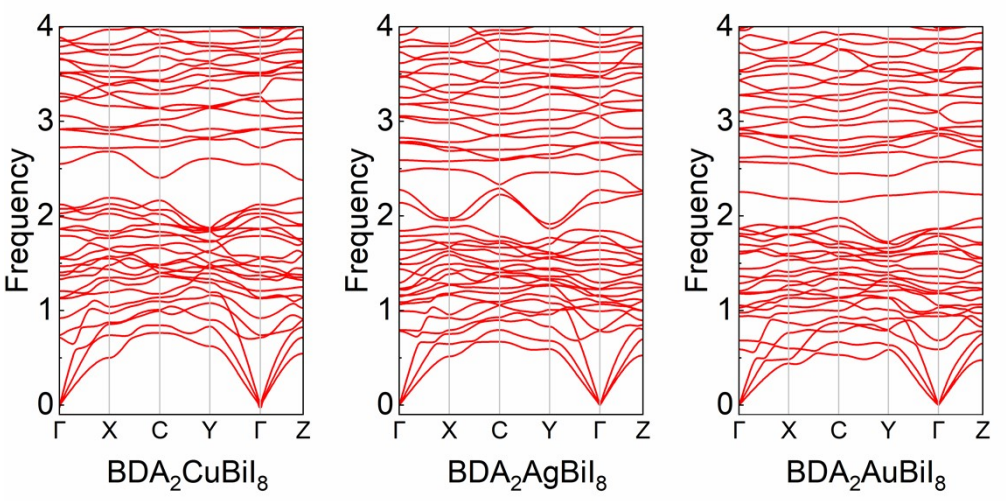

Fig. S18. Phonon band structures of $BDA_2(Cu/Ag/Au)BiI_8$.

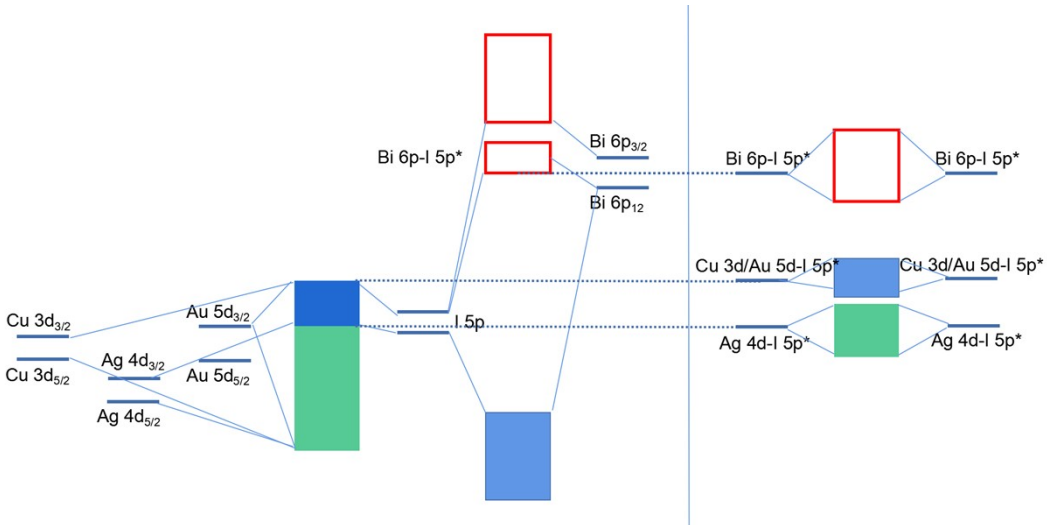

Fig. S19. Estimated molecular orbital bonding diagram of BDA_2CuBiI_8, BDA_2AgBiI_8, and BDA_2AuBiI_8.

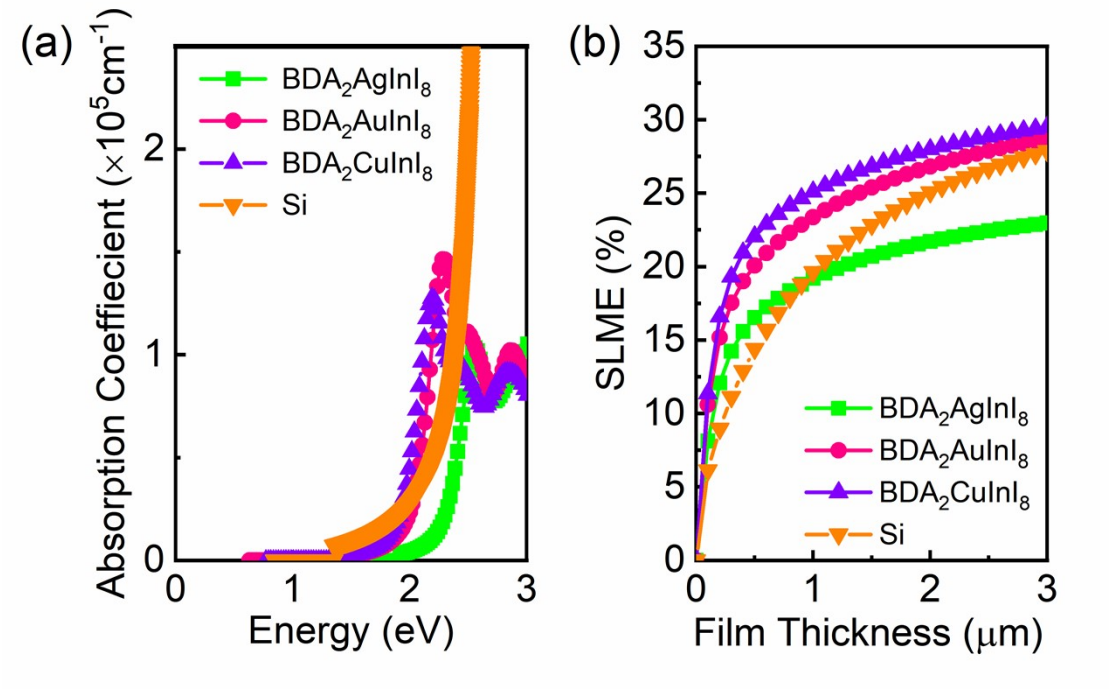

Fig. S20. (a) Calculated absorption spectrum of $BDA_2Cu/Ag/AuInI_8$ and Si; (b) Simulated spectroscopic limited maximum efficiency (SLME) of $BDA_2Cu/Ag/AuInI_8$ and Si.

Table S4. The calculated dielectric constants of 2D double perovskites $BDA_2M_IM_{III}Cl_8$ (M_I = Na^+, K^+, Rb^+, Cu^+, Ag^+, and Au^+; M_{III} = Bi^{3+}, In^{3+}, and Sb^{3+}) including the electron contribution (ε_∞) and the ionic contribution (ε_0); the effective masses of electrons (m_e^*) in the conduction band and holes (m_h^*) in the valence band; exciton binding energies, E_b (eV) in different directions.

Compounds	Direction	Dielectric Constants			Effective Mass		Exciton Binding Energies
	k	ε_∞	ε_0	ε_{std}	m_e^*	m_h^*	E_b
$BDA_2NaBiCl_8$	X	2.96	4.31	7.27	23.99	2.67	3.73
	Y	2.91	3.22	6.13	2.82	10.89	3.60
	Z	2.90	1.79	4.69	3.02	4.84	3.01
$BDA_2NaInCl_8$	X	2.84	4.36	7.20	1.7	3.74	1.97
	Y	2.77	7.21	9.98	1.14	4.12	1.58
	Z	2.75	1.93	4.68	2.78	4.34	3.05
$BDA_2NaSbCl_8$	X	3.01	6.34	9.35	5.73	5.42	4.18
	Y	2.96	4.15	7.11	1.6	3.82	1.75
	Z	2.94	3.66	6.60	3.37	3.57	2.73
BDA_2KBiCl_8	X	2.86	3.08	5.94	4.21	3.63	3.24
	Y	2.86	2.84	5.70	3.13	4.49	3.07
	Z	2.83	2.29	5.12	3.05	5.98	3.43
BDA_2KInCl_8	X	2.74	2.61	5.35	1.63	24.32	2.77
	Y	2.72	2.13	4.85	1.19	29.74	2.10
	Z	2.70	1.76	4.46	3.3	1.35	1.79
BDA_2KSbCl_8	X	2.91	4.13	7.04	3.37	5.39	3.33
	Y	2.89	3.84	6.73	2.75	2.88	2.29
	Z	2.88	2.66	5.54	2.56	23.99	3.79
$BDA_2RbBiCl_8$	X	2.81	2.81	5.62	3.21	6.87	3.77
	Y	2.82	4.62	7.44	3.25	15.08	4.57
	Z	2.79	1.90	4.69	3	1.16	1.46
$BDA_2RbInCl_8$	X	2.69	2.65	5.34	1.49	10.36	2.45
	Y	2.69	2.43	5.12	1.14	20.86	2.03
	Z	2.66	1.95	4.61	3.36	1.03	1.52
$BDA_2RbSbCl_8$	X	2.86	2.72	5.58	2.84	2.89	2.38
	Y	2.87	3.90	6.77	3.34	2.38	2.29
	Z	2.84	2.05	4.89	2.23	29.2	3.49
$BDA_2CuBiCl_8$	X	3.61	7.53	11.14	1.17	0.69	0.45
	Y	3.54	4.35	7.89	0.94	0.71	0.44
	Z	3.07	2.56	5.63	4.46	54.61	5.95
$BDA_2CuInCl_8$	X	3.38	7.36	10.74	2.22	1.88	1.21
	Y	3.28	6.81	10.09	0.79	1.72	0.68

	Z	2.92	1.24	4.16	2.18	18.56	3.11
$BDA_2CuSbCl_8$	X	3.73	13.56	17.29	1.42	0.63	0.43
	Y	3.66	6.63	10.29	0.98	0.65	0.40
	Z	3.11	2.43	5.54	5.48	23.71	6.26
$BDA_2AgBiCl_8$	X	3.29	4.54	7.83	1.98	0.73	0.67
	Y	3.24	4.07	7.31	1.32	0.74	0.61
	Z	3.04	2.74	5.78	5.17	30.36	6.50
$BDA_2AgInCl_8$	X	3.13	3.35	6.48	4.35	1.49	1.54
	Y	3.05	2.76	5.81	2.01	1.43	1.22
	Z	2.92	1.83	4.75	2.11	4.5	2.29
$BDA_2AgSbCl_8$	X	3.44	7.38	10.82	2.91	0.67	0.63
	Y	3.37	8.31	11.68	1.41	0.68	0.55
	Z	3.11	2.35	5.46	6.94	13.26	6.41
$BDA_2AuBiCl_8$	X	3.23	5.56	8.79	1.42	0.56	0.52
	Y	3.17	3.64	6.81	1.10	0.58	0.51
	Z	3.05	2.73	5.78	5.04	18.71	5.82
$BDA_2AuInCl_8$	X	3.07	3.76	6.83	3.92	1.35	1.45
	Y	2.99	2.79	5.78	0.76	1.23	0.71
	Z	2.92	1.54	4.46	2.45	11.80	3.24
$BDA_2AuSbCl_8$	X	3.36	5.75	9.11	1.96	0.49	0.47
	Y	3.30	0.92	4.22	1.08	0.52	0.44
	Z	3.10	3.49	6.59	5.75	9.95	5.16

Table S5. The calculated dielectric constants of 2D double perovskites $BDA_2M_IM_{III}Br_8$ (M_I = Na^+, K^+, Rb^+, Cu^+, Ag^+, and Au^+; M_{III} = Bi^{3+}, In^{3+}, and Sb^{3+}) including the electron contribution (ε_∞) and the ionic contribution (ε_0); the effective masses of electrons (m_e^*) in the conduction band and holes (m_h^*) in the valence band; exciton binding energies, E_b (eV) in different directions.

Compounds	Direction	Dielectric Constants			Effective Mass		Exciton Binding Energies
	k	ε_∞	ε_0	ε_{std}	m_e^*	m_h^*	E_b
$BDA_2NaBiBr_8$	X	3.38	3.68	7.06	16.31	3.76	3.64
	Y	3.31	2.90	6.21	3.16	6.21	2.60
	Z	3.28	1.60	4.88	2.37	3.33	1.75
$BDA_2NaInBr_8$	X	3.23	4.05	7.28	1.83	1.75	1.17
	Y	3.14	3.41	6.55	0.96	9.78	1.21
	Z	3.10	1.74	4.84	1.73	19.3	2.25
$BDA_2NaSbBr_8$	X	3.45	4.98	8.43	5.11	5.15	2.93
	Y	3.38	11.10	14.48	1.17	4.01	1.08
	Z	3.34	2.47	5.81	1.99	1.97	1.21
BDA_2KBiBr_8	X	3.22	3.11	6.33	3.8	4.06	2.57
	Y	3.21	3.31	6.52	2.17	9.78	2.34
	Z	3.19	1.71	4.90	1.52	1.35	0.96
BDA_2KInBr_8	X	3.08	2.28	5.36	1.62	14.87	2.09
	Y	3.05	2.53	5.58	1.01	16.69	1.39
	Z	3.01	1.96	4.97	2.24	1.12	1.12
BDA_2KSbBr_8	X	3.28	3.25	6.53	3.07	5.3	2.46
	Y	3.26	2.66	5.92	2.26	3.75	1.80
	Z	3.24	2.31	5.55	1.19	2.14	0.99
$BDA_2RbBiBr_8$	X	3.14	3.43	6.57	2.92	6	2.71
	Y	3.15	3.52	6.67	2.22	11.29	2.54
	Z	3.11	2.30	5.41	1.58	0.83	0.77
$BDA_2RbInBr_8$	X	3.00	2.61	5.61	1.45	12.24	1.96
	Y	2.98	2.61	5.59	0.98	16.13	1.41
	Z	2.95	1.63	4.58	2.31	0.75	0.88
$BDA_2RbSbBr_8$	X	3.20	6.33	9.53	2.74	2.07	1.57
	Y	3.20	3.21	6.41	2.93	2.76	1.89
	Z	3.17	3.18	6.35	1.12	6.33	1.29
$BDA_2CuBiBr_8$	X	4.63	7.94	12.57	0.68	0.47	0.18
	Y	4.51	8.54	13.05	0.55	0.49	0.17
	Z	3.50	1.63	5.13	2.24	9.43	2.01

$BDA_2CuInBr_8$	X	4.33	3.66	7.99	1.1	1.17	0.41
	Y	4.21	4.79	9.00	0.5	1.13	0.27
	Z	3.33	1.61	4.94	1.35	6.15	1.36
$BDA_2CuSbBr_8$	X	4.94	11.29	16.23	0.8	0.45	0.16
	Y	4.80	8.18	12.98	0.59	0.48	0.16
	Z	3.56	2.21	5.77	3.65	6.21	2.47
$BDA_2AgBiBr_8$	X	3.76	4.91	8.67	1.07	0.56	0.35
	Y	3.69	2.91	6.60	0.75	0.57	0.32
	Z	3.34	3.19	6.53	2.33	3.58	1.72
$BDA_2AgInBr_8$	X	3.76	4.02	7.78	13.67	1.04	0.93
	Y	3.64	3.27	6.91	0.5	1.05	0.35
	Z	3.31	2.27	5.58	1.39	2.01	1.02
$BDA_2AgSbBr_8$	X	4.16	7.42	11.58	1.33	0.55	0.31
	Y	4.08	10.21	14.29	0.83	0.56	0.27
	Z	3.55	2.83	6.38	3.31	2.95	1.68
$BDA_2AuBiBr_8$	X	4.04	3.67	7.71	0.72	0.36	0.20
	Y	3.95	3.46	7.41	0.55	0.38	0.20
	Z	3.46	2.11	5.57	2.2	5.16	1.75
$BDA_2AuInBr_8$	X	3.74	4.13	7.87	1.28	0.77	0.47
	Y	3.62	4.51	8.13	0.46	0.74	0.29
	Z	3.29	4.21	7.50	1.51	4.31	1.41
$BDA_2AuSbBr_8$	X	4.24	6.49	10.73	1.02	0.35	0.20
	Y	4.14	5.61	9.75	0.62	0.37	0.18
	Z	3.52	3.06	6.58	2.83	3.4	1.70

Table S6. The calculated dielectric constants of 2D double perovskites $BDA_2M_IM_{III}I_8$ (M_I = Na^+, K^+, Rb^+, Cu^+, Ag^+, and Au^+; M_{III} = Bi^{3+}, In^{3+}, and Sb^{3+}) including the electron contribution (ε_∞) and the ionic contribution (ε_0); the effective masses of electrons (m_e^*) in the conduction band and holes (m_h^*) in the valence band; exciton binding energies, E_b (eV) in different directions.

Compounds	Direction	Dielectric Constants			Effective Mass		Exciton Binding Energies
	k	ε_∞	ε_0	ε_{std}	m_e^*	m_h^*	E_b
BDA_2NaBiI_8	X	4.10	4.96	9.06	5.12	2.73	1.44
	Y	4.07	3.50	7.57	1.67	2.89	0.87
	Z	3.99	2.01	6.00	0.99	4.39	0.69
BDA_2NaInI_8	X	3.98	5.27	9.25	5.1	2.05	1.26
	Y	3.90	3.70	7.60	0.98	3.69	0.69
	Z	3.80	1.94	5.74	0.97	5.2	0.77
BDA_2NaSbI_8	X	4.22	9.97	14.19	7.76	2.54	1.46
	Y	4.16	5.35	9.51	1.42	2.37	0.70
	Z	4.07	3.89	7.96	0.58	1.03	0.30
BDA_2KBiI_8	X	3.75	2.87	6.62	4.58	3.36	1.87
	Y	3.74	2.81	6.55	1.56	4.88	1.15
	Z	3.72	1.94	5.66	0.69	0.97	0.40
BDA_2KInI_8	X	3.73	3.44	7.17	2.77	14.83	2.28
	Y	3.71	3.36	7.07	0.97	7.86	0.85
	Z	3.64	1.79	5.43	1.4	0.95	0.58
BDA_2KSbI_8	X	3.95	4.91	8.86	3.25	2.83	1.32
	Y	3.94	3.53	7.47	2.88	3.81	1.44
	Z	3.93	3.69	7.62	0.44	1.03	0.27
BDA_2RbBiI_8	X	3.73	3.02	6.75	3.15	4.13	1.75
	Y	3.75	2.61	6.36	1.45	5.83	1.12
	Z	3.73	1.99	5.72	0.72	0.64	0.33
BDA_2RbInI_8	X	3.57	2.69	6.26	0.99	8.96	0.95
	Y	3.57	2.64	6.21	1.44	8.26	1.31
	Z	3.50	2.02	5.52	1.38	0.61	0.47
BDA_2RbSbI_8	X	3.80	3.66	7.46	2.91	3.72	1.54
	Y	3.81	3.32	7.13	2.94	4.59	1.68
	Z	3.79	3.00	6.79	0.44	0.63	0.25
BDA_2CuBiI_8	X	6.03	7.35	13.38	0.46	0.37	0.08
	Y	5.92	9.31	15.23	0.36	0.37	0.07
	Z	4.28	1.87	6.15	1.08	2.49	0.56

BDA_2CuInI_8	X	5.65	6.49	12.14	0.6	0.78	0.14
	Y	5.58	5.27	10.85	0.33	0.8	0.10
	Z	4.10	1.76	5.86	0.75	1.95	0.44
BDA_2CuSbI_8	X	5.76	7.22	12.98	0.53	0.35	0.09
	Y	5.69	4.82	10.51	0.37	0.37	0.08
	Z	4.45	1.51	5.96	1.82	1.8	0.62
BDA_2AgBiI_8	X	5.18	6.41	11.59	0.63	0.47	0.14
	Y	5.13	5.44	10.57	0.45	0.44	0.11
	Z	4.27	3.22	7.49	1.08	1.17	0.42
BDA_2AgInI_8	X	5.13	3.69	8.82	1.55	0.79	0.27
	Y	5.04	4.31	9.35	0.36	0.82	0.13
	Z	4.18	1.89	6.07	0.81	0.92	0.34
BDA_2AgSbI_8	X	5.45	7.44	12.89	1.65	0.46	0.16
	Y	5.39	6.94	12.33	0.6	0.46	0.12
	Z	4.35	4.40	8.75	1.01	1.05	0.37
BDA_2AuBiI_8	X	5.55	4.97	10.52	0.4	0.27	0.07
	Y	5.44	3.73	9.17	0.31	0.27	0.07
	Z	4.22	1.79	6.01	1.2	1.61	0.53
BDA_2AuInI_8	X	5.12	4.59	9.71	0.55	0.53	0.14
	Y	5.03	4.20	9.23	0.3	0.55	0.10
	Z	4.02	29.20	33.22	0.86	1.5	0.46
BDA_2AuSbI_8	X	6.03	8.44	14.47	1.54	0.26	0.08
	Y	5.90	15.10	21.00	0.87	0.28	0.08
	Z	4.33	11.03	15.36	0.58	1.27	0.29